Nonreciprocal acoustic transmission in space-time modulated coupled resonators

Chen Shen, Xiaohui Zhu, Junfei Li, and Steven A. Cummer

Phys. Rev. B **100**, 054302 — Published 6 August 2019
DOI: 10.1103/PhysRevB.100.054302

Nonreciprocal Acoustic Transmission in Space-Time Modulated Coupled Resonators

Chen Shen[1,*], Xiaohui Zhu[2,1], Junfei Li[1] and Steven A. Cummer[1,†]
[1] *Department of Electrical and Computer Engineering, Duke University, Durham, North Carolina 27708, USA*
[2] *School of Mechatronics Engineering, Harbin Institute of Technology, Harbin, Heilongjiang, 150001, China*
**chen.shen4@duke.edu* †*cummer@ee.duke.edu*
(Dated: July 16, 2019)

Systems that break reciprocity offer new possibilities for controlling wave propagation. Here we study the scattering properties of coupled resonator systems that are under dynamic modulation. Strong linear nonreciprocal transmission is manifested in the acoustic regime by introducing an initial spatial phase bias to the space-time modulated coupled resonators. A theoretical model is developed to characterize the system and the results are in good agreement with experimental observations. Our work opens up new opportunities for designing compact nonreciprocal devices and developing acoustic topological insulators.

The study of nonreciprocal scattering and directional control of wave power flow has received considerable recent research interest [1–7]. However, wave propagation in conventional media is generally reciprocal, which is a fundamental principle for any linear time-invariant systems without external bias [8]. Reciprocity can thus be broken by biasing time-odd quantities into the media. In electromagnetism and photonics, nonreciprocity has been achieved by using magnetic materials [9], employing nonlinearities [2, 10] or breaking time-reversal symmetry [11], and has sparked numerous fascinating applications. Successful demonstration of nonreciprocity in the field of acoustics, on the other hand, is much rarer [12].

To realize acoustic nonreciprocity, one approach to create the time-odd bias is to employ intrinsic time-reversal symmetry breaking by using passive or active nonlinearities [13–16]. The rectification rate, i.e., isolation level of one-way transportation can in principle be very high. However, this approach typically requires bulky and complicated structures and suffers from strong signal distortion. A high level of input energy is also needed in order to excite nonlinear effects. These constraints make it difficult to apply this technique in real world scenarios. For example, in many applications such as communication, linear nonreciprocity with unchanged frequency content is preferred which restrict the use of this method.

An alternative way to induce nonreciprocity is the use of external spatiotemporal modulation where the media properties or the interaction among different components are time dependent [4, 17–19]. This approach offers many design degrees of freedom manifested by the modulation parameters and can in principle be very efficient. Although there has been abundant demonstrations in photonic and electromagnetic systems based on this idea, it is much more difficult to realize it in the acoustic regime due to the lack of effective modulation techniques. Other than elastic waves [20, 21], most proposals to achieve acoustic nonreciprocity based on spatiotemporal modulations only exist in theory [22–26] or through pseudotime-varying modulation [27]. Experimental demonstrations based on space-time modulation have been primarily achieved by moving background medium [28, 29]. Their practical usage, on the other hand, is severely limited as the systems are complicated and are high energy-consuming.

Here we propose and experimentally demonstrate nonreciprocal acoustic transmission with space-time modulation in a coupled resonator system. By driving the resonators mechanically, the resonance frequencies of the individual resonators can be modulated dynamically. This not only provides an efficient means to induce space-time modulation in acoustics but also breaks the time reversal symmetry and imparts a strong spatial bias to the system. Although nonreciprocal acoustic propagation has been proposed using resonator systems [26], its efficiency is limited due to low transmission near the resonance frequency of the Helmholtz resonators [30]. In this work the resonators are acoustic cavities which feature transmission peak at resonance frequencies and the efficiency is greatly enhanced. Since the resonators are coupled, a small amount of modulation can result in strong interaction that leads to nonreciprocal responses. Nonreciprocal propagation in the structure is realized by suitably choosing the modulation parameters that are well within the experimental capabilities. Our work makes linear, compact, low energy-consuming acoustic diodes possible and can be useful for applications in acoustic communications, etc.

Consider a two-level coupled resonator system as shown in Fig. 1, the two resonators have their resonance frequencies ω_1 and ω_2, and are connected to external ports 1 and 2 with lifetimes $\tau_1 = 1/\gamma_1$ and $\tau_2 = 1/\gamma_2$. γ_1 and γ_2 are the decay rates of the resonators. The coupling strength is κ and is assumed to be constant under small modulations. The states of the two resonators are written as:

$$|\psi\rangle = \begin{bmatrix} \alpha_1(t) \\ \alpha_2(t) \end{bmatrix}. \quad (1)$$

Under time modulation with frequency Ω, $\alpha_{1,2}(t)$ can

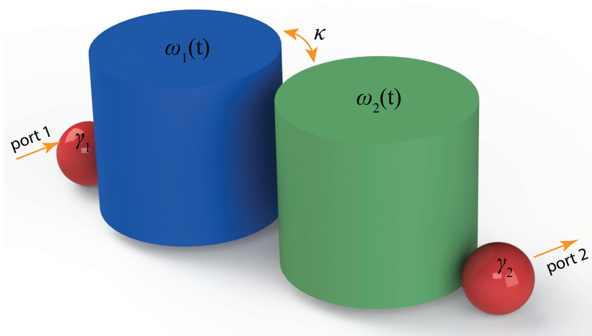

FIG. 1. Schematic diagram of the system under study. The resonance frequencies of the two coupled resonators (with coupling strength κ) are modulated dynamically. The resonators are connected to external ports with lifetimes $1/\gamma_1$ and $1/\gamma_2$.

be expressed as summations of different harmonics using temporal coupled mode theory [31–33]:

$$\alpha_{1,2}(t) = \sum a^n_{1,2} e^{j(\omega_{1,2}+n\Omega)t} \tag{2}$$

where $a^n_{1,2}$ are the complex amplitude coefficients of the nth harmonic of the two resonators.

The states $|\psi\rangle$ satisfy a Schrödinger type differential equation:

$$-j\partial_t|\psi\rangle = \mathcal{H}|\psi\rangle + s(t) \tag{3}$$

where $\mathcal{H}$ is the Hamiltonian operator and is written as:

$$\mathcal{H} = \begin{bmatrix} \omega_1(t) + j\gamma_1 & \kappa \\ \kappa & \omega_2(t) + j\gamma_2 \end{bmatrix}. \tag{4}$$

$s(t)$ is the source with an incident field from the external ports. Consider a harmonic excitation from port 1, $s(t)$ is written as:

$$s(t) = \begin{bmatrix} \sqrt{2\gamma_1} e^{j\omega t} \\ 0 \end{bmatrix} \tag{5}$$

with ω being the excitation frequency.

We consider a sinusoidal modulation of the two resonators, in which the resonance frequencies $\omega_{1,2}(t)$ are written as:

$$\begin{aligned} \omega_1(t) &= \omega_0 + \delta\omega\cos(\Omega t) \\ \omega_2(t) &= \omega_0 + \delta\omega\cos(\Omega t + \phi), \end{aligned} \tag{6}$$

where $\delta\omega$ is the modulation depth, ϕ is the initial phase difference of modulation. Although the theory can be generally applied to two arbitrary resonators, here the two resonators are considered identical in the static case, i.e., $\omega_{1,2} = \omega_0$ without modulation. The decay rates are also assumed to be the same for the two resonators, i.e., $\gamma_1 = \gamma_2 = \gamma$.

Insert the above equations into Eq. (3), the follwing equations can be obtained:

$$(\omega + n\Omega - \omega_0 - j\gamma)a^n_1 - \frac{\delta\omega}{2}(a^{n+1}_1 + a^{n-1}_1) - \kappa a^n_2 = \sqrt{2\gamma_1}\delta_{n0} \tag{7}$$

$$(\omega + n\Omega - \omega_0 - j\gamma)a^n_2 - \frac{\delta\omega}{2}(a^{n+1}_2 e^{-j\phi} + a^{n-1}_2 e^{j\phi}) - \kappa a^n_1 = 0 \tag{8}$$

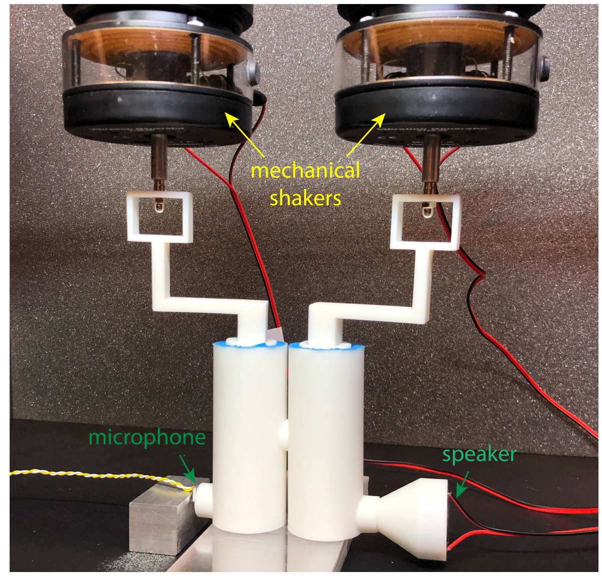

FIG. 2. Experimental setup of the coupled resonators under modulation. A speaker is used to excite the system and the response is recorded by a microphone. Mechanical shakers are connected to the cavities to dynamically modulate their effective lengths.

Here δ is the Kronecker delta. Equations (7) and (8) can be solved by truncating higher order harmonics. For example, under weak modulation, i.e., $\delta\omega/\omega_0 \ll 1$, only first few harmonics need to be considered. Here the first 50 harmonics are included in our calculations, which is sufficient to yield accurate results (see Supplemental Material [34]). The reflected/transmitted amplitudes at ports 1 and 2 of each harmonic are then obtained by multiplying $a_{1,2}$ with $\sqrt{2\gamma_{1,2}}$. Here we are interested in nonreciprocal transmission in the linear regime and the scattering properties of the fundamental mode are defined as S_{21} in the forward direction (corresponds to high transmission) and S_{12} in the backward direction (corresponds to low transmission).

It is noted that the theoretical framework can in principle be applied to any coupled resonator system in different physical scenarios. In this work we aim at its realization in acoustics. Figure 2 shows the experimental setup of the system. Two cylindrical cavities are chosen as the resonators. They are identical with radius and height being 15 mm and 88 mm, respectively. Here we use the second eigenmode of the cavity which possesses maximum pressure amplitude at its center [35]. The two cavities are effectively coupled through a hole opened at their centers. The radius and length of the coupling hole are 4 mm and 10 mm, respectively, which ensures a sufficient coupling strength between the cavities, as will be

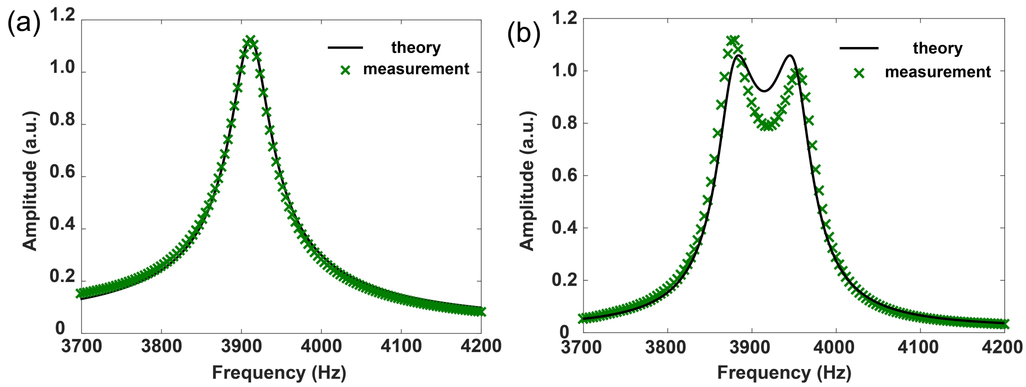

FIG. 3. Measured system response in the static case. (a) Measured pressure spectrum of a single resonator for the determination of decay rate. (b) Measured pressure spectrum of a coupled resonator pair for the determination of coupling strength.

shown later. In practice, the coupling strength can be tuned by modifying the radius of the coupling hole or adding additional holes along the cavities [35]. Two external ports with a 5 mm radius are opened at one end of each cavity. A loudspeaker is connected to one of the external ports using a customized 3D printed adapter to excite the system. Sinusoidal waves with a duration of 1s are used for the measurements and the response is recorded at a 4 Hz step. The opening of the cavities is connected to a Nitrile rubber coated disk to ensure good seal of the cavity while maintaining flexibility. The disks are further connected to mechanical shakers (model SF-9324) for dynamic modulation.

Towards this end, experiments are carried out in the static case, i.e., without activating the mechanical shakers, to determine the coupling strength κ and decay rate γ of the resonators. The coupling port is first blocked and a microphone (type ADMP401) is inserted through a slit on top of the cavity [36] to measure the pressure of a single resonator. The decay rate is then determined by fitting the measured data according to the analytically predicted onsite spectrum $|P_s(\omega)| = A|\frac{1}{\omega-(\omega_0+j\gamma)}|$, where A is the amplitude coefficient [37]. Figure 3a depicts the measured pressure amplitude of a single cavity and the decay rate is determined to be $\gamma = 21.8$ Hz. To obtain the coupling strength between the two resonators, a Green's function approach is adopted [35, 37]. The analytically obtained spectrum is expressed as $|P_c(\omega)| = A|\langle p|\overleftrightarrow{G}(\omega)|s\rangle|$ for the coupled resonator pair. Here $\overleftrightarrow{G}(\omega)$ is the Green's function of the system, $|s\rangle$ and $|p\rangle$ are the basis vectors and are written as $(1,0)^T$. The coupling between the resonators is manifested by the separation of the peaks in the spectrum. By comparing this separation with the measured curve as shown in Fig. 3b, the value of κ can be obtained and is found to be $\kappa = 37.5$ Hz. The peaks of the measured response have small variations, which may be caused by the slight geometrical difference between the cavities and unbalanced excitations.

The experimentally determined coupling strength and decay rate are then plugged into the theory above to find the optimal modulation parameters. As the mechanical shakers have larger vibration amplitudes at lower frequencies, here we set their working frequency to be $\Omega = 50$ Hz so that a few millimeter modulation depth can be delivered. The isolation ratio $20\log|S_{21}/S_{12}|$ and transmission asymmetry $|S_{21}| - |S_{12}|$ [38] are plotted in Fig. 4 as a function of $\delta\omega$ and ϕ. It can be observed that the isolation ratio can be as high as 80 dB with maximum transmission asymmetry being around 0.7. This indicates that the coupled resonator system under dynamic modulation can yield strong nonreciprocity with a relatively low insertion loss by suitably choosing the modulation parameters. The parameters chosen to be implemented in our experiments are marked by the stars in Fig. 4 by balancing the isolation ratio and transmission asymmetry, which read $\delta\omega = 74$ Hz and $\phi = 78°$.

Next we demonstrate nonreciprocal transmission with dynamic modulation by activating the mechanical shakers. A function generator (RIGOL DG4202) is used to generate the signals and an audio amplifier (type PAM8403) is employed to drive the shakers. Since the modulation produces some noises that exceed the dynamic range of the original microphone when measuring, another microphone (type BJ-21590-000) is used which has larger dynamic range but slightly less sensitivity. We note that the noise mainly comes from friction between moving components and can be reduced by ensuring better contact. The microphone is secured on a metallic block and is not in contact with the resonators to isolate vibrations. As the modulation depth $\delta\omega$ is expressed in terms of frequency, it needs to be translated to the actual displacement delivered by the shakers. This can be done by analyzing the eigenfrequencies of the cavity modes (see Supplemental Material [34]). The effective length of the cavities need to be varied from 86.1 mm to 89.5 mm and a maximum displacement of 3.4 mm is required, which can be fulfilled by the shakers. Accurate modulation is ensured by a high-speed camera, which measures the displacement of the disks at the end of the cavities (see Supplemental Material [34]). The calculated

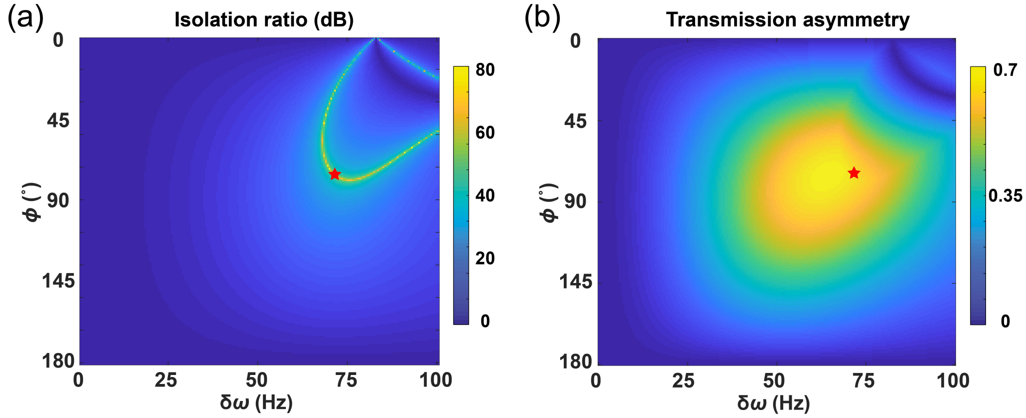

FIG. 4. Scattering properties of the coupled resonator system. Isolation ratio $20\log|S_{21}/S_{12}|$ (a) and transmission asymmetry $|S_{21}|-|S_{12}|$ (b) as a function of modulation depth $\delta\omega$ and initial phase difference ϕ. The parameters implemented in experiments are marked by the stars.

initial phase difference of $\phi = 78°$ is applied to measure the transmission in one direction and the positions of the speaker and the microphone are interchanged to measure the transmission from the other direction.

Figure 5 shows the measured pressure spectrum of the structure. Good agreement can be observed between the theory and the experiment, which unambiguously demonstrates the nonreciprocal effect. The small variation patterns in the spectrum is well captured by the measurements. The small discrepancies can be attributed to the inherent microphone errors (finite size, noise, etc.) and imperfect modulation produced by the mechanical shakers. A 50 Hz band of around 6 dB isolation emerges near the resonance frequency, which is relatively narrow and is typical for such coupled resonator systems [23, 39]. Larger bandwidth may be achieved by increasing the decay rate of the resonators and further optimizing the modulation parameters. Maximum isolation occurs at the resonance frequency at 3908 Hz, which aligns well with measurements, and an isolation ratio of 19.9 dB is observed.

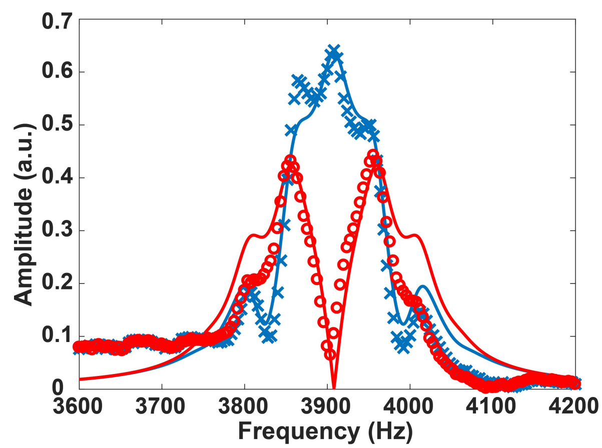

FIG. 5. Experimental demonstration of nonreciprocal transmission using space-time modulated coupled resonators. The solid curves represent theoretical calculations and the measurement data is denoted by the markers. Blue: forward direction; red: backward direction.

To conclude, we have theoretically developed and experimentally demonstrated a compact acoustic diode based on space-time modulated resonators. The resonators are driven mechanically and the initial phase of modulation creates the time-odd bias that is essential to achieve nonreciprocal transmission. An isolation ratio of nearly 20 dB is observed in experiments and the measured system response is in good agreement with theoretical predictions. Our work provides a feasible route to achieve linear acoustic nonreciprocal device that embraces space-time modulation and does not require external moving fluid. The coupled resonator system proposed here can be readily extended to host a larger number of resonators for the realization of subwavelength circulators [23] or Floquet topological insulators [24]. The system could therefore be a good candidate for the experimental exploration of space-time modulation in the field of acoustics. Since topological states [40, 41] and exceptional points [42, 43] can be easily introduced in coupled resonator structures, our work may also be useful for the study of these effects in a dynamic fashion. The theory outlined here is generic to wave physics and the dimensions of the resonators can be scaled for nonreciprocal sound propagation at other frequencies. It is hoped that the design could serve as basic elements for various acoustic applications.

ACKNOWLEDGMENTS

This work was supported by a Multidisciplinary University Research Initiative grant from the Office of Naval Research (Grant No. N00014-13-1-0631) and an Emerging Frontiers in Research and Innovation grant from the National Science Foundation (Grant No. 1641084).

[1] K. Fang, Z. Yu, and S. Fan, Realizing effective magnetic field for photons by controlling the phase of dynamic modulation, Nature photonics **6**, 782 (2012).

[2] Y. Shi, Z. Yu, and S. Fan, Limitations of nonlinear optical isolators due to dynamic reciprocity, Nature photonics **9**, 388 (2015).

[3] J. Kim, M. C. Kuzyk, K. Han, H. Wang, and G. Bahl, Non-reciprocal brillouin scattering induced transparency, Nature Physics **11**, 275 (2015).

[4] D. L. Sounas and A. Alù, Non-reciprocal photonics based on time modulation, Nature Photonics **11**, 774 (2017).

[5] C. Caloz, A. Alù, S. Tretyakov, D. Sounas, K. Achouri, and Z.-L. Deck-Léger, Electromagnetic nonreciprocity, Physical Review Applied **10**, 047001 (2018).

[6] D. Torrent, O. Poncelet, and J.-C. Batsale, Nonreciprocal thermal material by spatiotemporal modulation, Physical review letters **120**, 125501 (2018).

[7] S. A. Mann, D. L. Sounas, and A. Alù, Nonreciprocal cavities and the time–bandwidth limit, Optica **6**, 104 (2019).

[8] J. Strutt, Some general theorems relating to vibrations, Proceedings of the London Mathematical Society **1**, 357 (1871).

[9] J. D. Adam, L. E. Davis, G. F. Dionne, E. F. Schloemann, and S. N. Stitzer, Ferrite devices and materials, IEEE Transactions on Microwave Theory and Techniques **50**, 721 (2002).

[10] B. Peng, Ş. K. Özdemir, F. Lei, F. Monifi, M. Gianfreda, G. L. Long, S. Fan, F. Nori, C. M. Bender, and L. Yang, Parity–time-symmetric whispering-gallery microcavities, Nature Physics **10**, 394 (2014).

[11] L. Chang, X. Jiang, S. Hua, C. Yang, J. Wen, L. Jiang, G. Li, G. Wang, and M. Xiao, Parity–time symmetry and variable optical isolation in active–passive-coupled microresonators, Nature photonics **8**, 524 (2014).

[12] R. Fleury, D. Sounas, M. R. Haberman, and A. Alu, Nonreciprocal acoustics, Acoustics Today **11**, 14 (2015).

[13] B. Liang, B. Yuan, and J.-c. Cheng, Acoustic diode: Rectification of acoustic energy flux in one-dimensional systems, Physical review letters **103**, 104301 (2009).

[14] B. Liang, X. Guo, J. Tu, D. Zhang, and J. Cheng, An acoustic rectifier, Nature materials **9**, 989 (2010).

[15] N. Boechler, G. Theocharis, and C. Daraio, Bifurcation-based acoustic switching and rectification, Nature materials **10**, 665 (2011).

[16] B.-I. Popa and S. A. Cummer, Non-reciprocal and highly nonlinear active acoustic metamaterials, Nature communications **5**, 3398 (2014).

[17] F. Ruesink, M.-A. Miri, A. Alu, and E. Verhagen, Nonreciprocity and magnetic-free isolation based on optomechanical interactions, Nature communications **7**, 13662 (2016).

[18] K. Fang, J. Luo, A. Metelmann, M. H. Matheny, F. Marquardt, A. A. Clerk, and O. Painter, Generalized nonreciprocity in an optomechanical circuit via synthetic magnetism and reservoir engineering, Nature Physics **13**, 465 (2017).

[19] D. B. Sohn, S. Kim, and G. Bahl, Time-reversal symmetry breaking with acoustic pumping of nanophotonic circuits, Nature Photonics **12**, 91 (2018).

[20] Y. Wang, B. Yousefzadeh, H. Chen, H. Nassar, G. Huang, and C. Daraio, Observation of nonreciprocal wave propagation in a dynamic phononic lattice, Physical review letters **121**, 194301 (2018).

[21] G. Trainiti, Y. Xia, J. Marconi, G. Cazzulani, A. Erturk, and M. Ruzzene, Time-periodic stiffness modulation in elastic metamaterials for selective wave filtering: Theory and experiment, Physical Review Letters **122**, 124301 (2019).

[22] D.-D. Dai and X.-F. Zhu, An effective gauge potential for nonreciprocal acoustics, EPL (Europhysics Letters) **102**, 14001 (2013).

[23] R. Fleury, D. L. Sounas, and A. Alù, Subwavelength ultrasonic circulator based on spatiotemporal modulation, Physical Review B **91**, 174306 (2015).

[24] R. Fleury, A. B. Khanikaev, and A. Alu, Floquet topological insulators for sound, Nature communications **7**, 11744 (2016).

[25] J. Li, C. Shen, X. Zhu, Y. Xie, and S. A. Cummer, Nonreciprocal sound propagation in space-time modulated media, Physical Review B **99**, 144311 (2019).

[26] C. Shen, J. Li, Z. Jia, Y. Xie, and S. A. Cummer, Nonreciprocal acoustic transmission in cascaded resonators via spatiotemporal modulation, Physical Review B **99**, 134306 (2019).

[27] Y.-X. Shen, Y.-G. Peng, D.-G. Zhao, X.-C. Chen, J. Zhu, and X.-F. Zhu, One-way localized adiabatic passage in an acoustic system, Physical Review Letters **122**, 094501 (2019).

[28] R. Fleury, D. L. Sounas, C. F. Sieck, M. R. Haberman, and A. Alù, Sound isolation and giant linear nonreciprocity in a compact acoustic circulator, Science **343**, 516 (2014).

[29] Y. Ding, Y. Peng, Y. Zhu, X. Fan, J. Yang, B. Liang, X. Zhu, X. Wan, and J. Cheng, Experimental demonstration of acoustic chern insulators, Physical Review Letters **122**, 014302 (2019).

[30] J. Li, X. Zhu, C. Shen, X. Peng, and S. A. Cummer, Transfer matrix method for the analysis of space-time modulated media and systems, arXiv preprint arXiv:1905.10658 (2019).

[31] S. Fan, W. Suh, and J. D. Joannopoulos, Temporal coupled-mode theory for the fano resonance in optical resonators, JOSA A **20**, 569 (2003).

[32] J. D. Joannopoulos, S. G. Johnson, J. N. Winn, and R. D. Meade, *Photonic Crystals: Molding the Flow of Light* (Princeton Univ. Press, Princeton, NJ, 2008).

[33] T. T. Koutserimpas and R. Fleury, Nonreciprocal gain in non-hermitian time-floquet systems, Physical review letters **120**, 087401 (2018).

[34] See supplemental material at [url] for convergence of the theoretical model, eigenfrequency analysis of the cavity modes and experimental apparatus., .

[35] K. Ding, G. Ma, Z. Zhang, and C. Chan, Experimental demonstration of an anisotropic exceptional point, Physical review letters **121**, 085702 (2018).

[36] C. Shen, J. Li, X. Peng, and S. A. Cummer, Synthetic exceptional points and unidirectional zero reflection in non-hermitian acoustic systems, Physical Review Materials **2**, 125203 (2018).

[37] K. Ding, G. Ma, M. Xiao, Z. Zhang, and C. T. Chan, Emergence, coalescence, and topological properties of multiple exceptional points and their experimental re-

alization, Physical Review X **6**, 021007 (2016).
[38] A. Kamal, J. Clarke, and M. Devoret, Noiseless non-reciprocity in a parametric active device, Nature Physics **7**, 311 (2011).
[39] N. A. Estep, D. L. Sounas, J. Soric, and A. Alù, Magnetic-free non-reciprocity and isolation based on parametrically modulated coupled-resonator loops, Nature Physics **10**, 923 (2014).
[40] H. Xue, Y. Yang, F. Gao, Y. Chong, and B. Zhang, Acoustic higher-order topological insulator on a kagome lattice, Nature materials **18**, 108 (2019).
[41] X. Ni, M. Weiner, A. Alù, and A. B. Khanikaev, Observation of higher-order topological acoustic states protected by generalized chiral symmetry, Nature materials **18**, 113 (2019).
[42] V. Achilleos, G. Theocharis, O. Richoux, and V. Pagneux, Non-hermitian acoustic metamaterials: Role of exceptional points in sound absorption, Physical Review B **95**, 144303 (2017).
[43] R. El-Ganainy, K. G. Makris, M. Khajavikhan, Z. H. Musslimani, S. Rotter, and D. N. Christodoulides, Non-hermitian physics and pt symmetry, Nature Physics **14**, 11 (2018).